Modeling Biconical Antennas

L. B. Cebik, W4RNL

In its purest form, the biconical antenna--usually a dipole--consists of two half elements in the form of cones joined at the center, the feedpoint, at the vertex of each cone. Practical versions of the antenna take a number of forms, some of which appear in **Fig. 1**. By far the most popular form simulates a cone by using several linear wires symmetrically arranged. Called the "phantom biconical" antenna by Kraus, the wires might have loose ends (usually) or they might have a perimeter wire connecting the outer ends. In VHF or UHF service, the individual wires or rods might screw into a hub/feedpoint, allowing for rapid assembly and disassembly at field sites.

Fig. 1

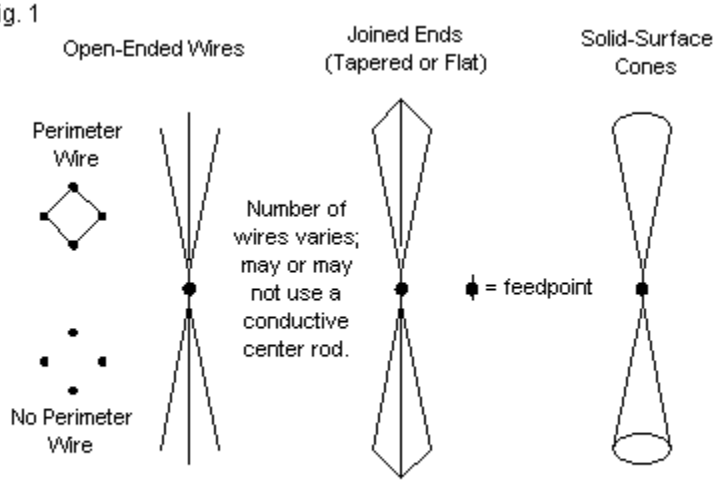

Some Biconical Configurations Used at VHF and UHF

The center sketch shows the elements rejoined at the far end of the centerline. Although the sketch hints at 4 wires, actual versions tend to use 6 or 8 wires per end. We shall have occasion to discuss the function of the tapered outer ends, especially as they contrast with a flat closed end. In principle, the number of rods may range from 2 (creating the familiar fan-element dipole) up to an indefinitely large number. However, the number of rods ceases to show any improvement in performance at around 6 or so, depending upon the diameter of the rods. The final sketch shows actual solid-surface cones. This form usually appears only in the UHF spectrum, where solid surfaces are as economical as individual rods.

The biconical dipole has existed for a very long time, since it originated in fundamental antenna theory as it relates to treating the antenna as an extension of the transmission line. In principle, selecting the correct angle for each conical section would provide a constant impedance along the dipole legs. Although many texts provide the basic theoretical foundations of infinitely long biconical sections, among introductory texts, Kraus provides the most significant information on biconical antennas with finite lengths. See Chapter 8 of the second edition of *Antennas*. For a full treatment of the mathematics behind the biconical antenna, see S. A. Schelkunoff's 1952 book, *Advanced Antenna Theory*, and subsequent technical papers refining the calculations.

The biconical dipole remained simply one antenna design among many until the 1960s and MIL-STD-461, which provided standards for electro-magnetic compatibility (EMC) testing and laid down a usable and practical biconical antenna design for use at frequencies from 20 through 300 MHz. (See also applicable CISPR and ANSI standards.) In practice, standard biconical antennas became ultra-wide-band (UWB) antennas. There are many incarnations available from a plethora of makers. They range in power handling capabilities from 1 watt to several kilowatts.

These notes on the biconical antenna do not attempt to add anything to what we know about the biconical antenna shape. Instead, they have another purpose. In NEC, we must use a rod structure within the model, since solid surfaces are not feasible. However, NEC models work within some constraints relative to the geometry of the antenna. For greatest accuracy, the feedpoint or source wire should contain 3 segments to ensure that the current on each adjacent segment to the source segment is equal. In addition, the segment lengths on each wire of the total antenna should be approximately equal. Furthermore, the angles at a junction of wires should be wide enough so that the center portions of each element do not interpenetrate.

When comparing models using different structures to capture the same overall physical geometry, the average gain test (AGT) is the normal measure for determining the most adequate model. (Adequacy here is internal to NEC models as a general measure of the reliability of the output data. It does not itself certify that the physical antenna will replicate the data in actual performance tests. However, in most cases, the more ideal the AGT value, the closer the model will come to reflecting actual antenna performance for models that do not press the well-published limits of NEC calculations.)

Therefore, my goal is to identify to the degree possible any modeling issues within NEC that may pertain to the modeling of biconical antennas. We shall uncover a few along the way. In fact, we shall develop 2 different ways of modeling the biconical dipole and note the limitations of each method. We shall record (and adjust as necessary) gain figures as a check against anticipated reality. In addition, for comparison among the models, we shall record the 2:1 SWR bandwidth of each version using the resonant impedance of the model as a reference. These numbers are less predictors of reality than they are a means of comparing modeling techniques, a means that goes beyond the fundamental AGT test. We shall also have occasion to explore the expanded SWR curves of many of the versions in the search to locate the second low-impedance resonant frequency.

The Basic Biconical Models

Because it is convenient to do so, we shall look at both closed-end and open-end versions of the biconical dipole. The closed-end models will use element extensions that meet at the extreme point of the center line to form a flat end, that is, an end surface 90° to the center line. (We shall look at tapered ends later.)

Each modeling progression will begin with 2-wire fan structures and survey several angles between the centerline and the actual wires of the element. Selectively, we shall then proceed to 4-wire and 6-wire cone simulations. The design frequency will be 299.7925 MHz, so that all entries can be read metrically or as fractions of a wavelength. The wires will be perfect (that is, lossless), and the environment will be free-space. All biconical dipoles will extend along the Z-axis so that modeling elevation patterns will yield E-plane plots of the antenna's far field. The wire diameter is 2 mm (0.002 m) to provide a realistic dimension while avoiding excessive pressure on the NEC angular junction limitation. The results of modeling progressions for

closed and open biconicals will appear in separate tables (**Table 1** and **Table 2**). However, the entries in the tables require some explanation in advance.

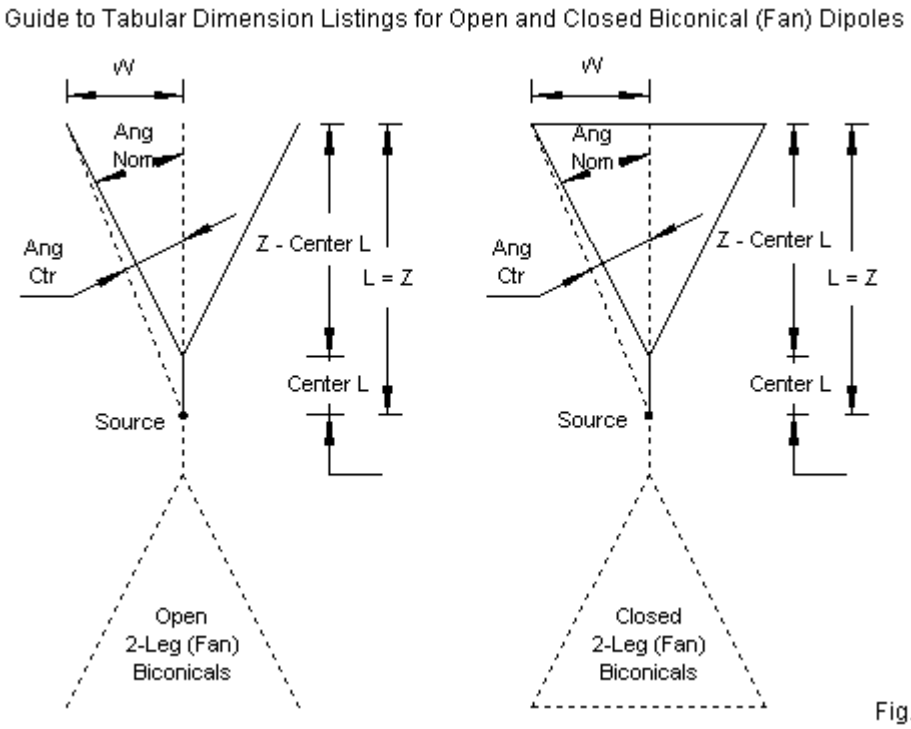

Fig. 2

Since the model's geometry will have considerable import, **Fig. 2** provides a guide to the dimensional entries of each table. All dimensions are half-lengths, that is, they apply to one-half of the dipole structure. "L=Z" gives the total half-length of the element. "Center L" provide the half-length of the center section that is parallel to the centerline, prior to division into the cone-simulating wires. The dimension labeled "Z-Center L" gives the length of the conical section along the Z-axis. "Len" supplies the length of each rod that marks the simulated conical surface. "W" is the distance from the centerline to the tip of the rods. It is also the length of the wires forming the closed end of one set of models.

The physical structure of the models yields 2 angles of note. "Ang nom" is the nominal design angle and is close to the angle between the dipole centerline and each rod. The angles within the models are very close to the nominal angle, since in most cases, one can vary the value of both "L" and "W" together to preserve the initial design angle. The angle may vary slightly in some cases due to the need to make slight adjustments to obtain resonance within +/- j1 Ω. "Ang Ctr" is the angle between the dipole centerline and the outer limits of the cone as measured from the origin of the geometry coordinate system. This angle may vary slightly from the nominal angle as a function of the length of "Center L." As a reference that includes all relevant lengths, the tables also include a "Path" entry. This entry provides the total (half) length including the center length, the rod length, and (for closed-end models) the return wire length (that is, Center L, Len, and sometimes W).

For reasons that will become apparent as we examine the modeling data, I developed a second method of modeling the biconical structures. To prevent the junction of the angled wires from yielding inadequate models due to segment interpenetration, I offset center wires 0.007m

from the centerline. Each center wire connects only to cone-forming wires equally offset from the centerline. Therefore, each part of the structure has only three wires, and the angles of the end wires to the center wire are relatively shallow. **Fig. 3** shows the general scheme.

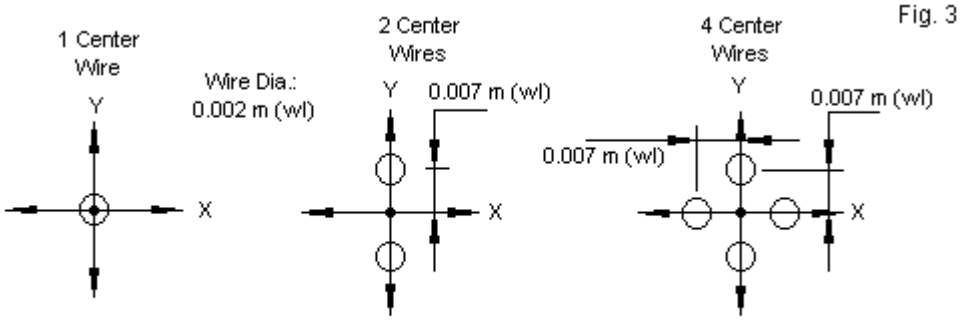

Fig. 3

Model Layouts for Different Center-Wire Arrangements Looking Down (or Up) Z-Axis

Although the sketch stops with a square of 4 center wires, the models use up to 6 wires. The structure of the center wires is partially responsible for limiting the study to 6-wire conical sections. With 6 center wires, each individual wire is 0.007-m apart, since each pair of center wires form an equilateral triangle with the Z-axis. Moving to 8-wires would have reduced the spacing between center wires and potentially exceeded NEC recommendations that parallel wires be spaced apart by several radii.

The method of feeding the cone is straightforward. One center wire serves as the feedpoint (on the center segment of the three). From this wire, a NEC transmission line (TL) extends to each remaining center wire's middle segment. Each line is very short (0.001 m) to form a virtual short circuit. Under these conditions, the impedance of the TL is non-critical, so I used 75 Ω. The line is connected in normal (that is, not in reverse) fashion. The result is a parallel feed to all center wires.

The effect of parallel feeding separate center wires largely overcomes the potential problem of segment interpenetration at angular junctions. However, it effectively increases the diameter of the center section of each modeled biconical dipole. Therefore, we should not expect corresponding single-wire and multiple-wire models to behave identically. The absence of a true identity will make it somewhat more difficult to separate differences that are due to modeling technique from those that are due to simulated physical differences between models. However, the alternative of thickening the single center wire would have yielded potentially larger difficulties.

Now we may turn to **Table 1**, which lists the results for the open-ended models in the survey. As a reference point in examining the performance data for the models, we may use a resonant center-fed 1/2-λ dipole. The wire is 0.002-m perfect material at the test frequency of 299.7925 MHz in free-space. The required length for resonance is 0.474-m (half-length: 0.237 m), and the resonant impedance is 71.75 - j0.43 Ω. The reported gain is 2.13 dBi. More significantly for the tables to follow is the 2:1 SWR bandwidth using the resonant impedance as a reference. The bandwidth extends from 285 to 319 MHz, a 34-MHz spread for a bandwidth of just over 11%.

For each total number of legs, the table collects the information on all rod angles for each method of construction. Therefore, the section on 2-leg or fan models covers the single center

wire cases followed by the 2-center-wire cases. The table follows similar procedures for 4-leg and 6-leg models.

2-Leg (V-Fans)									4-Leg				6-Leg	Table 1
Type	Open	Open	Open	Open	Open	Open	Open	Open	Open	Open	Open	Open	Open	Open
Ang-nom	45	30	20	10	45	30	20	10	20	10	20	10	10	10
Ctr wires	1	1	1	1	2	2	2	2	1	1	4	4	1	6
Center L	0.0156	0.014	0.0098	0.00376	0.027	0.027	0.027	0.027	0.0088	0.0029	0.027	0.027	0.0027	0.027
L=Z	0.1601	0.1884	0.2017	0.2101	0.1655	0.1955	0.2086	0.2185	0.1742	0.1876	0.1869	0.2012	0.178	0.194
Z-Ctr L	0.1445	0.1744	0.1919	0.20634	0.1385	0.1685	0.1816	0.1915	0.1654	0.1847	0.1599	0.1742	0.1753	0.167
Len	0.207	0.202	0.2043	0.2095	0.202	0.1955	0.193	0.194	0.176	0.1875	0.17	0.1765	0.178	0.169
W	0.1483	0.1019	0.07	0.0364	0.154	0.1061	0.07	0.0379	0.06	0.0324	0.0647	0.0351	0.0309	0.0335
Ang-ctr	42.8	28.4	19.1	9.8	42.9	28.5	18.6	9.8	19	9.8	19.1	9.9	9.8	9.8
Path	0.2226	0.216	0.2141	0.2133	0.229	0.2225	0.22	0.221	0.1848	0.1904	0.197	0.2035	0.1807	0.196
AGT	0.999	1.000	1.000	0.999	0.999	0.999	1.000	1.001	1.060	1.001	1.003	1.000	1.012	1.002
AGT-gn	0	0	0	0	-0.01	0	0	0	0.25	0	0.01	0	0.05	0.01
Gain-bs	2.03	2.06	2.07	2.07	2.04	2.08	2.1	2.11	2.19	2.01	1.98	2.04	2.04	2.04
Gain-edge	1.39	1.74	1.91	2.03	1.37	1.73	1.92	2.05	2.19	2.01	1.98	2.04	2.04	2.04
Adj gn bs	2.03	2.06	2.07	2.07	2.05	2.08	2.1	2.11	1.94	2.01	1.97	2.04	1.99	2.03
Feed R	33.88	46.7	53.98	59.51	37.85	51.52	58.59	64.87	41.36	51.74	51.86	60.43	48.52	59.29
Feed X	-0.84	0.45	0.67	-0.38	0.6	-0.19	-0.62	-0.11	-0.67	-0.16	0.06	-0.16	0.4	0.86
SWR Ref	34	47	54	60	38	52	59	65	42	51	52	60	49	59
2:1-low	287	282.5	280.5	280.5	284	281	280	274	280	280	275.5	275.5	279.5	274
2:1-high	316	320	322.5	324	317	323	326	326	325.5	325	330	332	325.5	334
SWR BW	29	37.5	42	43.5	33	42	46	52	45.5	45	54.5	56.5	46	60
BW %	9.7	12.5	14.0	14.5	11.0	14.0	15.3	17.3	15.2	15.0	18.2	18.8	15.3	20.0
Notes:	Test frequency 299.7925; all dimension values = meters = wavelengths													
	All wires 0.002 m = 0.002 wl	L and W are half-lengths related to modeling conventions centered on coordinate system origin												
	All models use lossless (perfect) wire in a free-space environment													
	2-wire center sections: wires are 0.007m(wl) from Z-axis; one wire = source, other connected by a 0.001-m(wl) 75-Ohm TL (= short)													
	Open = loose or unterminated, unjoined wire ends													

The first notable item in the tables occurs with the single center wire models. As the nominal angle of the wires decreases, so too does the required length of the center wire needed to obtain an acceptable AGT score (ideally 1.000). In some cases, even with judiciously selected center wire lengths, a near perfect score (.995<AGT<1.005) is not possible. As well, the total wire segment length becomes shorter than the minimum recommended segment length. Finally, the center wire length becomes very critical, with only small changes yielding large changes in the AGT score.

In contrast, all of the multi-wire center section models use the same center length (although a different length is required for open-end and for closed-end models). Moreover, the length is not as critical within the model as the single center wire. The AGT changes very slowly with small changes in the center length. Finally, the segment length falls well within NEC guidelines relative to the wire diameter and the frequency of operation. (To determine the segment length from the tabulated data, double the half-length shown and divide by 3.)

Some general trends in the performance predicted by the models are consistent for both types of center sections. The 2-wire or fan models show differences in the gain for the fan broadside and the fan edge. The tables provide both numbers, but only corrects for the broadside gain. When the number of legs increases to 4, the antenna is symmetrical and the broadside-vs.-edge difference disappears. Another consistent factor is the improvement of the 2:1 SWR bandwidth as the angle between legs decreases. Maximum bandwidth falls in the region between about 20° and 10°. One consequence of this trend is to allow the use of fewer complex models as we increase the number of legs. The 4-leg models use only 20° and 10°, while the 6-leg models use only 10° as the nominal angle.

The same trends that we just saw for the open-ended biconical models also apply to the closed flat-end versions in **Table 2**. All closed multi-center-wire models use a constant length for the center wires, while the single-wire versions require a reduction in the center-wire length as the angle between wires decreases. The same sensitivities and insensitivities also apply to

these flat-end closed biconical antennas. We also find parallel trends in the performance data. In both tables, we may note of the 10° models that we find very little improvement in any performance category as we raise the number of legs from 4 to 6. In addition to modeling limitations noted earlier, extending the table with models using 8 or more legs appears otiose, although some commercial open-end wide-angle biconical antennas use up to 12 rods on each side of the feedpoint.

2-Leg (V-Fans)									4-Leg				6-Leg	Table 2
Type	Closed	Closed	Closed	Closed	Closed	Closed	Closed	Closed	Closed	Closed	Closed	Closed	Closed	Closed
Ang-nom	45	30	20	10	45	30	20	10	20	10	20	10	10	10
Ctr wires	1	1	1	1	2	2	2	2	1	1	4	4	1	6
Center L	0.013	0.011	0.009	0.0036	0.018	0.018	0.018	0.018	0.0088	0.0028	0.018	0.018	0.0027	0.018
L=Z	0.1185	0.1485	0.1685	0.191	0.13	0.158	0.178	0.1995	0.154	0.176	0.169	0.19	0.1696	0.185
Z-Ctr L	0.1055	0.1375	0.1595	0.1874	0.112	0.14	0.16	0.1815	0.1452	0.1732	0.151	0.172	0.1669	0.167
Len	0.169	0.159	0.1697	0.1903	0.1488	0.1574	0.1679	0.1835	0.1546	0.1759	0.1584	0.174	0.1695	0.169
W	0.1065	0.079	0.058	0.033	0.105	0.079	0.058	0.034	0.053	0.0305	0.055	0.0335	0.0294	0.0335
Ang-ctr	45.3	28	19	9.8	38.9	26.6	18	9.7	19	9.8	18	10	9.8	10.3
Path	0.2885	0.249	0.2367	0.2269	0.2718	0.2544	0.2439	0.2355	0.2164	0.2092	0.2314	0.2255	0.1976	0.2205
AGT	1.000	1.006	1.012	0.998	1.000	0.999	0.999	1.004	1.083	0.997	0.997	1.001	1.028	0.999
AGT-gn	0	0.02	0.05	-0.01	0	0	0	0.02	0.35	-0.01	-0.01	0	0.12	-0.01
Gain-bs	2.05	2.08	2.11	2.06	2.1	2.08	2.08	2.12	2.29	1.99	1.97	2.05	2.11	2.03
Gain-edge	1.56	1.81	1.97	2.02	1.6	1.8	1.93	2.12	2.29	1.99	1.97	2.05	2.11	2.03
Adj gn bs	2.05	2.06	2.06	2.07	2.1	2.08	2.08	2.1	1.94	2	1.98	2.05	1.99	2.04
Feed R	30.01	42.69	50.35	58.66	36.12	48.98	57.27	64.14	39.81	51.57	52.72	60.97	47.57	59.74
Feed X	0.41	0.07	-0.15	-0.17	0.67	0.87	0.73	0.36	0.04	-0.63	-0.39	0.66	-0.21	0.83
SWR Ref	30	43	50	59	36	49	57	64	40	52	53	61	48	60
2:1-low	287	284	282	282	285	281	280	279	280	280	275	275	280	273
2:1-high	314	320	321	319	316	321	324.5	325.5	320	325	334	332.5	326	335
SWR BW	27	36	39	37	31	40	44.5	46.5	40	45	59	57.5	46	62
BW %	9.0	12.0	13.0	12.3	10.3	13.3	14.8	15.5	13.3	15.0	19.7	19.2	15.3	20.7
Notes:	Test frequency 299.7925; all dimension values = meters = wavelengths													
	All wires 0.002 m = 0.002 wl	L and W are half-lengths related to modeling conventions centered on coordinate system origin												
	All models use lossless (perfect) wire in a free-space environment													
	2-wire center sections: wires are 0.007m(wl) from Z-axis; one wire = source, other connected by a 0.001-m(wl) 75-Ohm TL (= short)													
	Open = loose or unterminated, unjoined wire ends													

One impression left by commercial implementations of the biconical dipole is that bringing the ends back together at an angle may make a difference to the electrical performance of the antenna. To see if models would show such a difference, I created two additional single-center-wire models with 2 legs and a 20° angle between the centerline and the leg. In the first model, I increased the centerline length by a small amount. In the second, I increased it to approximate a constant radius formed by the junction of wires and the legs. **Fig. 4** shows a dimensional guide to the new models. L1 is the Z coordinate of the leg, while L2 is the total length along the Z-axis to the junction of the wires.

Guide to Tabular Dimension Listings
for Tapered Closed Biconical (Fan) Dipoles

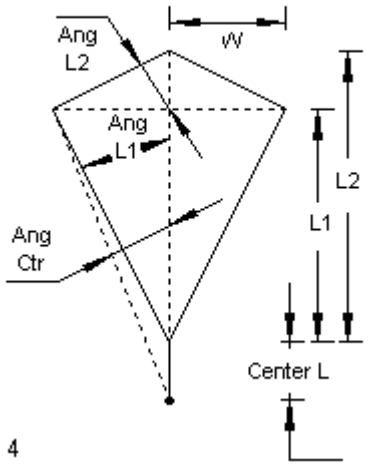

Fig. 4

We may compare the dimensional and performance data for the flat-end original model and the 2 additional models in **Table 3**. With respect to performance, there is no difference among the three models. In fact, there is almost no difference in the key parts of the model geometry. The center sections are almost identical. As well, we find only a small variation in the total path length from the feedpoint to the junction at the outer end of the dipole. Electrically, there appears to be no significant reason for choosing one geometry over another.

2-Leg (V-Fans): Tapered			Table 3
Type	Flat	Taper 1	Taper 2
Ang-nom	20	20	20
Ctr wires	1	1	1
Center L	0.009	0.0089	0.0089
L1=Z1	0.1685	0.168	0.165
L2=Z2	0.1685	0.173	0.179
Len1	0.1697	0.1784	0.1662
W1	0.058	0.057	0.057
Len 2	0.058	0.0572	0.0587
Ang-L1	29	19.7	20.1
Ang-L2	0	5	13.8
Path	0.2367	0.2445	0.2338
AGT	1.012	1.013	1.013
AGT-gn	0.05	0.06	0.06
Gain-bs	2.11	2.11	2.12
Gain-edge	1.97	1.97	1.98
Adj gn bs	2.06	2.05	2.06
Feed R	50.35	50.82	51.09
Feed X	-0.15	-0.29	-0.1
SWR Ref	50	51	51
2:1-low	282	282	282
2:1-high	321	321	321
SWR BW	39	39	39
BW %	13.0	13.0	13.0
Notes:	Test frequency 299.7925		
	All wires 0.002 m = 0.002 wl		
	Free-space, lossless wire		
	Taper 1 = small extension		
	Taper 2 = extension to the		
	approximate conical radius		

Because no electrically significant differences appeared in these models, I did not pursue these variations any further. The modeling data suggest that the major reasons for using a tapered closed end over either an open end or a flat end are likely mechanical. I can see that a tapered junction would allow one to adjust a prototype to resonance without wire pruning. Changing the centerline length of the tapered-end array would alter the resonant frequency more rapidly than it would change the wire angle to the centerline, thus allowing adjustment without changing the effective bandwidth. In addition, if we replace the solid connection at the change of angle in the wire with a hinge, we can create an element that collapses into a thinner linear structure for easy transport. Finally, with a fixed junction, the tapered-end closed biconical antenna likely has greater dimensional stability than an open-end or even a flat-end version of the antenna. One further aspect of the use of biconical antennas in EMC testing adds to the catalog of reasons for using this configuration. The basic design for most commercial EMC biconical dipoles replicates the original specifications in MIL-STD-461 from the

1960s. Hence, we find basic antennas from numerous makers with nearly identical lengths (1.35 to 1.40 m), all using roughly the same wire angles at each end. As we shall later note, the main differences between offerings lie in the feedpoint region.

We have not exhausted the comparison of alternative models of the biconical dipole. Let's draw together some directly comparable data for 2-, 4-, and 6-leg models for the 10° versions of the antenna using a single center wire and multiple center wires. **Table 4** does the work that allows use to examine more closely corresponding information. The table's left side shows open-ended models, while the right side shows closed-end versions. In each case, the single-wire and multi-wire center versions appear side-by-side. The progression of data for each column is the same as in the earlier tables.

1-Center Wire vs. N Center Wires												
	2-Leg		4-Leg		6-Leg		2-Leg		4-Leg		6-Leg	Table 4
Type	Open	Open	Open	Open	Open	Open	Closed	Closed	Closed	Closed	Closed	Closed
Ang-nom	10	10	10	10	10	10	10	10	10	10	10	10
Ctr wires	1	2	1	4	1	6	1	2	1	4	1	6
Center L	0.00376	0.027	0.0029	0.027	0.0027	0.027	0.0036	0.018	0.0028	0.018	0.0027	0.018
L=Z	0.2101	0.2185	0.1876	0.2012	0.178	0.194	0.191	0.1995	0.176	0.19	0.1696	0.185
Z-Ctr L	0.20634	0.1915	0.1847	0.1742	0.1753	0.167	0.1874	0.1815	0.1732	0.172	0.1669	0.167
Len	0.2095	0.194	0.1875	0.1765	0.178	0.169	0.1903	0.1835	0.1759	0.174	0.1695	0.169
W	0.0364	0.0379	0.0324	0.0351	0.0309	0.0335	0.033	0.034	0.0305	0.0335	0.0294	0.0335
Ang-ctr	9.8	9.8	9.8	9.9	9.8	9.8	9.8	9.7	9.8	10	9.8	10.3
Path	0.2133	0.221	0.1904	0.2035	0.1807	0.196	0.2269	0.2355	0.2092	0.2255	0.1976	0.2205
AGT	0.999	1.001	1.001	1.000	1.012	1.002	0.998	1.004	0.997	1.001	1.028	0.999
AGT-gn	0	0	0	0	0.05	0.01	-0.01	0.02	-0.01	0	0.12	-0.01
Gain-bs	2.07	2.11	2.01	2.04	2.04	2.04	2.06	2.12	1.99	2.05	2.11	2.03
Gain-edge	2.03	2.05	2.01	2.04	2.04	2.04	2.02	2.12	1.99	2.05	2.11	2.03
Adj gn bs	2.07	2.11	2.01	2.04	1.99	2.03	2.07	2.1	2	2.05	1.99	2.04
Feed R	59.51	64.87	51.74	60.43	48.52	59.29	58.66	64.14	51.57	60.97	47.57	59.74
Feed X	-0.38	-0.11	-0.16	-0.16	0.4	0.86	-0.17	0.36	-0.63	0.66	-0.21	0.83
SWR Ref	60	65	51	60	49	59	59	64	52	61	48	60
2:1-low	280.5	274	280	275.5	279.5	274	282	279	280	275	280	273
2:1-high	324	326	325	332	325.5	334	319	325.5	325	332.5	326	335
SWR BW	43.5	52	45	56.5	46	60	37	46.5	45	57.5	46	62
BW %	14.5	17.3	15.0	18.8	15.3	20.0	12.3	15.5	15.0	19.2	15.3	20.7
Notes:	See Tables 1 and 2											

With the open-end models, the differences between the path lengths of each center type are small and consistent. However, with the closed-end models, the long path length required by the multi-wire centers increases more rapidly as the number of legs increases. The path length partially compensates for the required differences in the length of the center sections between the single-wire and the multi-wire models, but obviously, the compensation is incomplete. Moreover, the larger effective diameter of the multi-wire centers does not fully account for the differences from the single-center-wire versions, since there are differentials between open and closed versions of the antenna. As a consequence, the table provides us with a view of at least one limitation of either type of model adequately to capture biconical antenna behavior.

More evident from just a brief examination of the performance data reports is the fact that multi-wire center models show a consistently wider SWR bandwidth than models with a single center wire. Although the table allows detailed comparisons, **Fig. 5** illustrates the differences for 2- and 4-leg models having closed ends.

Whether the ends are open or joined, the differential in SWR bandwidth is a function of the number of legs forming the simulation of the cone. However, once a relatively complete cone is formed with 4 or 6 wires, the change in differential disappears, but the basic difference remains between models with a single center wire and models using multiple center wires. Once more, the models are not self-explanatory in accounting for the difference. The center sections are

short enough (with a maximum length of just over 10% of the total model length in the extreme cases) so that the increased effective diameter of the multi-wire center sections does not provide a complete explanation. As well, in no model in the series does the AGT value change by more than 0.001 from one end of the SWR passband to the other. In fact, one might examine the current tables to determine why each model yields the SWR passband that emerges. However, such accounts do not themselves offer any reason for judging one type of model or the other as more reflective of actual antenna performance. The matter might be called trivial if the differentials were not so clear, consistent, and great.

Fig. 5

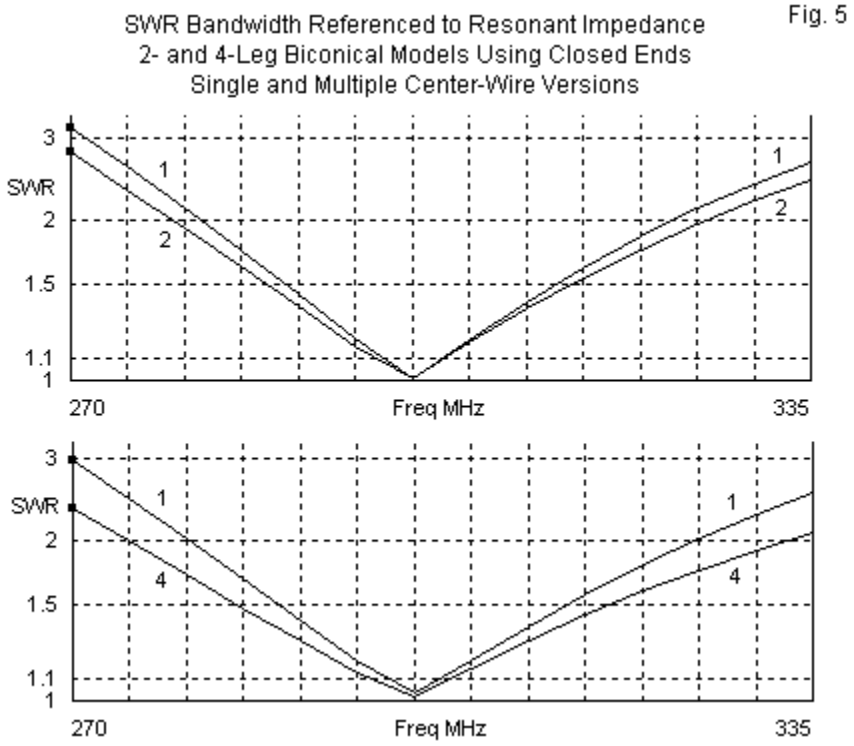

I noted in passing that we need not model past 4 or 6 legs to obtain a reasonable approximation of a full conical structure. To confirm this suggestion--and to note its limits--let's draw together the data for multi-wire center models of 4-leg and 6-leg 10° biconical antennas with both open and closed ends. For each number of legs, we may place side-by-side the data for open and closed end models. **Table 5** supplies the numbers.

The similarities in performance between open-end and closed-end versions for each leg count should be striking. For example, the feedpoint impedance values are almost identical. Moreover, the SWR passbands for each number of legs are virtually indistinguishable, as evidenced in **Fig. 6**.

Open vs. Closed Structure				Table 5
Multiple Center Wire Models				
	4-Leg		6-Leg	
Type	Open	Closed	Open	Closed
Ang-nom	10	10	10	10
Ctr wires	4	4	6	6
Center L	0.027	0.018	0.027	0.018
L=Z	0.2012	0.19	0.194	0.185
Z-Ctr L	0.1742	0.172	0.167	0.167
Len	0.1765	0.174	0.169	0.169
W	0.0351	0.0335	0.0335	0.0335
Ang-ctr	9.9	10	9.8	10.3
Path	0.2035	0.2255	0.196	0.2205
AGT	1.000	1.001	1.002	0.999
AGT-gn	0	0	0.01	-0.01
Gain-bs	2.04	2.05	2.04	2.03
Gain-edge	2.04	2.05	2.04	2.03
Adj gn bs	2.04	2.05	2.03	2.04
Feed R	60.43	60.97	59.29	59.74
Feed X	-0.16	0.66	0.86	0.83
SWR Ref	60	61	59	60
2:1-low	275.5	275	274	273
2:1-high	332	332.5	334	335
SWR BW	56.5	57.5	60	62
BW %	18.8	19.2	20.0	20.7
Notes:	See Tables 1 and 2			

Fig. 6

SWR Bandwidths Referenced to Resonant Impedance
4- and 6-Leg Biconical Models Using Multiple Center Wires
Open-End and Closed-End Versions

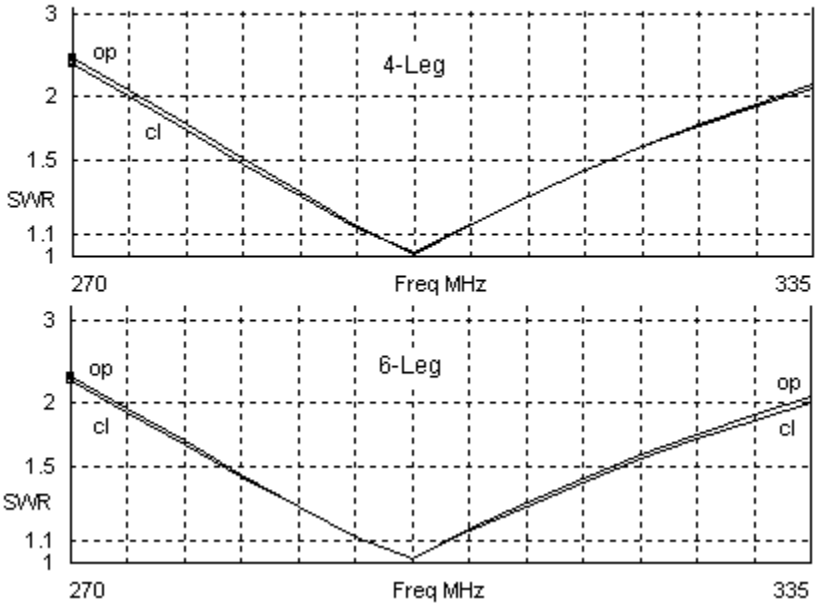

Equally apparent is the fact that a 6-leg model shows only a tiny increment of improved SWR performance over its 4-leg counterpart along with only a 1-Ω difference in the feedpoint

impedance. The latter difference would disappear within construction variables, and the former difference would be difficult to measure if we used the average of several implementations of each model. For the closed-end models, we find only a small difference between 4-leg and 6-leg path lengths. The difference in path length is more evident for open-end models, since the overall rod length decreases as we add rods to simulate the cone. Due to variables in the construction of the more complex models, we can reach no firm conclusions about dimensions. However, the performance similarities between open and closed versions of the multi-leg biconical simulation remain clear.

The Biconical Dipole as an Ultra-Wide-Band Antenna

In the field of EMC testing, the biconical antenna offers ultra-wide-band use. Typical 1.4-m versions of the antenna find use between 20 and 300 MHz. However, nothing in our models suggests anything more than a significant but limited widening of the SWR passband relative to our original reference dipole. **Fig. 7** compares the basic 2:1 SWR passbands of closed models with multiple center wires to show the maximum raw passband that we can expect. In each case, the curve is referenced to the resonant impedance of the model. The 6-leg model has nearly double the passband width of the reference dipole, but falls far shy of UWB status.

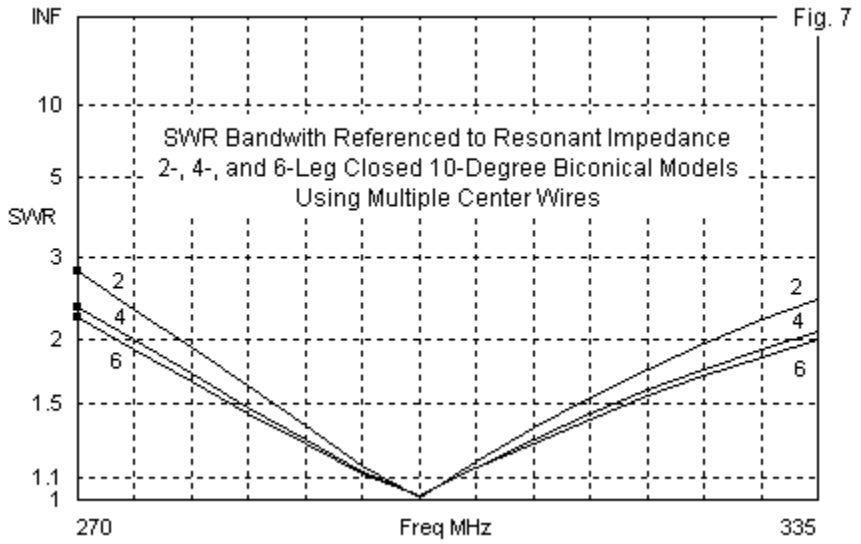

The operating range of EMC biconical antennas extends far beyond the limits of resonance. A 1.4-m biconical dipole would have a resonant impedance of about 85 MHz (give or take 5 to 10 MHz). An upper frequency limit of about 300 MHz or so would place the next low-impedance resonance at or near the useful limit in the specification sheets. However, we also must take into account the fact that the pattern changes as we operate an antenna at frequencies higher than the half-wavelength resonant frequency.

Fig. 8 shows some properties of a standard (linear) dipole's E-plane pattern as we change the operating frequency. The upper portion of the figure confirms what we all know, namely, that the pattern remains virtually unchanged throughout the normal 2:1 SWR passband. As we raise the operating frequency, the beam width narrows as we pass an effective dipole length of 1 λ. Beyond that point, we find the emergence of sidelobes. There is no known specification for the limit that we may set to the ratio of the main lobe strength to the sidelobe strength. Therefore, within this exercise, I arbitrarily set a limit of 10 dB. When the ratio of the main lobe

to the sidelobe passes this point, we may take a frequency reading. For the dipole, the frequency is about 760 MHz (using inexact visual inspection of the E-plane pattern). The lower right corner of the figure shows what happens if we continue to raise the operating frequency: the sidelobes come to dominate the pattern and the former main lobe falls in strength. We may for this exercise consider this type of radiation pattern to be unacceptable.

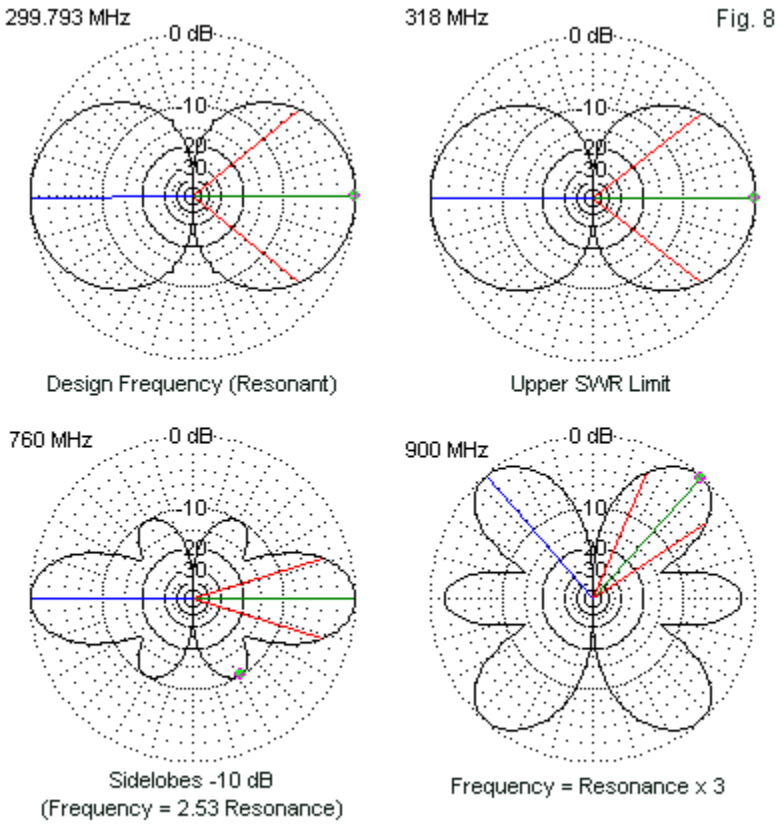

Typical Dipole Free-Space E-Plane Patterns
with Increasing Frequency Relative to Design Frequency

As an exercise, I explored the collection of biconical models to determine the frequency at which the sidelobes reached the -10-dB level. The results appear in **Table 6**. The data are for 2-, 4-, and 6-leg 10° models using open and closed versions as well as center sections with single and multiple wires. For reference, I also recorded the feedpoint impedance in each case. Since the visual means of determining the –10-dB level for the sidelobes has restricted precision, the data are rounded and approximate.

Although the multi-wire center section models showed wider SWR passbands than the corresponding models with a single wire at the center, the exploration of patterns shows an opposite trend. The models with a single wire at the center show higher frequencies at which the sidelobes reach the -10-dB level than models with multi-wire centers. The differential grows as we increase the number of leg wires. However, we do not find any major differences between open and closed models of each type of center section. The exercise reveals one more way in which the two modeling techniques yield different results of significant proportions without suggesting which technique is closer to physical reality.

Frequency Limit for -10-dB Sidelobe E-Plane Patterns							Table 6
		1 Center Wire			Multiple Center Wires		
Legs	Type	Freq MHz	Feed R	Feed X	Freq MHz	Feed R	Feed X
2	Closed	850	135	-230	810	100	-225
2	Open	850	150	-230	810	125	-240
4	Closed	925	175	-155	840	90	-155
4	Open	925	180	-155	850	100	-165
6	Closed	950	185	-130	850	75	-135
6	Open	950	190	-130	860	90	-150
Reference Dipole		760	145	-430			
Notes:	Frequencies rounded in 25-MHz increments						
	Impedances rounded in 5-Ohm increments						

The sidelobe limit frequency does not correspond to the frequency at which the antenna reaches its second low-impedance resonant point. That frequency for a linear dipole is generally slightly above 3 times the half-wavelength resonant frequency. **Fig. 9** compares the SWR curves (with the half-wavelength resonant impedance as a reference) for a linear dipole and one of the many-leg models.

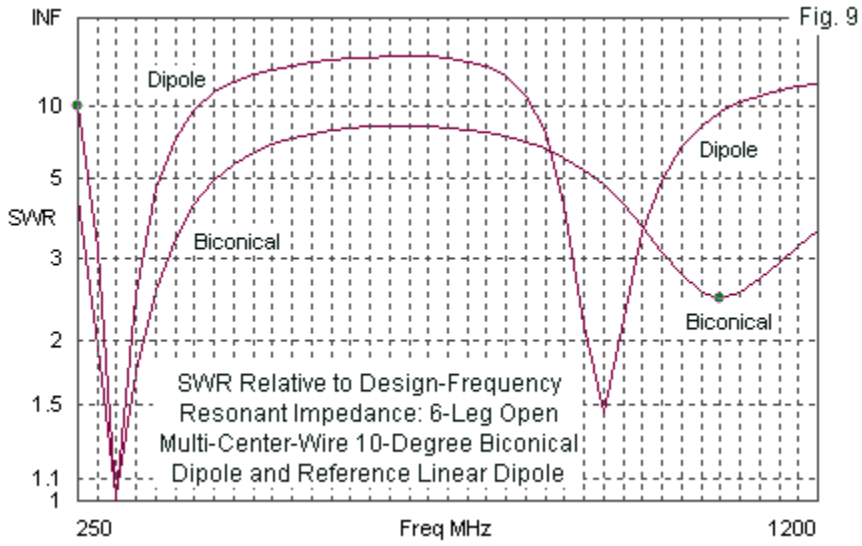

The second low-impedance resonance for the linear dipole occurs at about 925 MHz (using 25-MHz increments for the sweep). The comparable resonant frequency for the biconical dipole is about 1075 MHz. The increment between the -10-dB limit frequency and the second resonance frequency increases as we add legs to the biconical model.

Nevertheless, all of the frequencies at the sidelobe limit are very much higher than value shown by the reference linear dipole. Moreover, as we add legs to the biconical antenna models, the shape of the pattern changes at the upper frequency limit. **Fig. 10** provides patterns at the sidelobe-limit frequency for the linear dipole and for 2-, 4-, and 6-leg biconical dipole.

Fig. 10

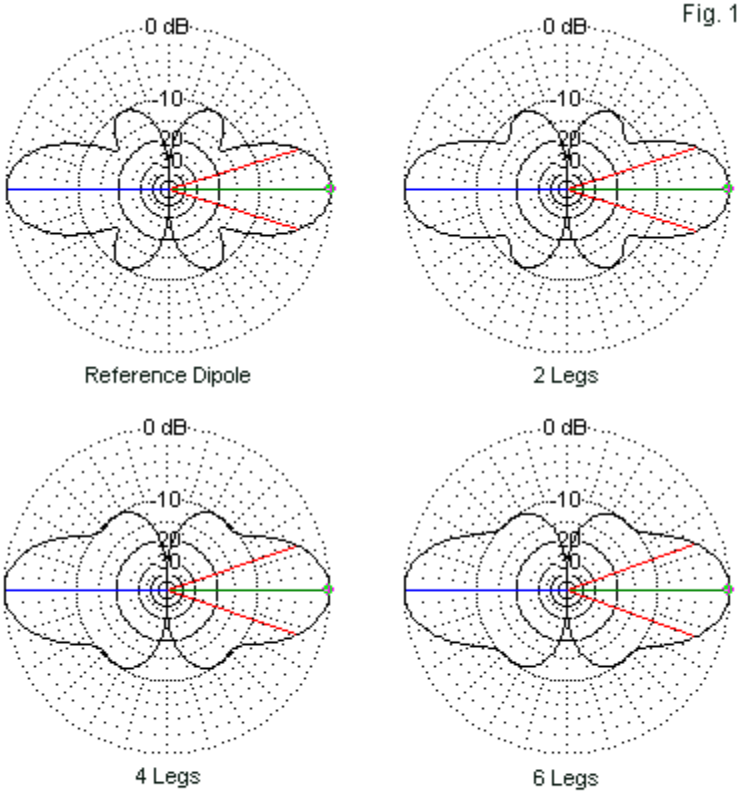

Typical Free-Space E-Plane Patterns for Biconical Models
at -10-dB Sidelobe-Limit Frequency with Various Leg Counts

As we increase the number of legs in these 10° models, the sidelobes change their shape. Although all models show a sidelobe peak at about 60° from the main lobe bearing, the null between lobes decreases in depth. Again, we find little difference between 4-leg and 6-leg models, but the progression to that level is evident from the remaining patterns in the illustration. The 6-leg pattern shows virtually no null between lobes but only a change in the rate of gain decrease as we move from the main lobe heading toward the deep 90° side null. Indeed, the pattern might remain usable at reduced gain for some frequency spread beyond the arbitrary limit that marks this exercise. (Since this part of our examination of models is using less precise limit-setting methods, introducing precise gain values would be inappropriate, especially in view of the unresolved priority of one modeling technique over the other. Nevertheless, the trends involved show up for all biconical models in the series.)

If the patterns are usable to a relatively high frequency, the remaining questions about the biconical antenna as an ultra-wide-band antenna is the SWR. Here, we can give only rough indications from the models at hand. In **Fig. 9**, we saw that the peak SWR level between low-impedance resonant points is much higher for a linear dipole than for the biconical model used to generate the curve. The difference may not be readily apparent on the log scale used to record the SWR. However, the dipole shows a peak source resistance of over 1500 Ω and a peak reactance of about -j850 Ω, allowing for the 25-MHz increments in the sweep. In contrast, the modeled biconical antenna shows a peak resistance of about 400 Ω and a peak reactance of about -j230 Ω. (See pages 351 to 353 of Kraus' *Antennas*, 2nd Ed. for background on biconical impedance levels between low-impedance resonant points.)

Although we have lower peak impedance levels at and near the so-called anti-resonance frequencies, the SWR curve for the biconical antenna in **Fig. 9** does not resemble typical SWR curves (usually referenced to 50 Ω) provided in the specifications sheets for biconical antennas intended for EMC testing. **Fig. 11** shows a pair of such curves for standard 1.4-m wire biconical antennas. One curve is for a low-power biconical antenna (1 watt), while the other curve derives from a high-power (>1 kilowatt) antenna. Not only are both curves quite disparate from the SWR curve for the biconical antenna in **Fig. 9**; they are equally different from each other.

Fig. 11

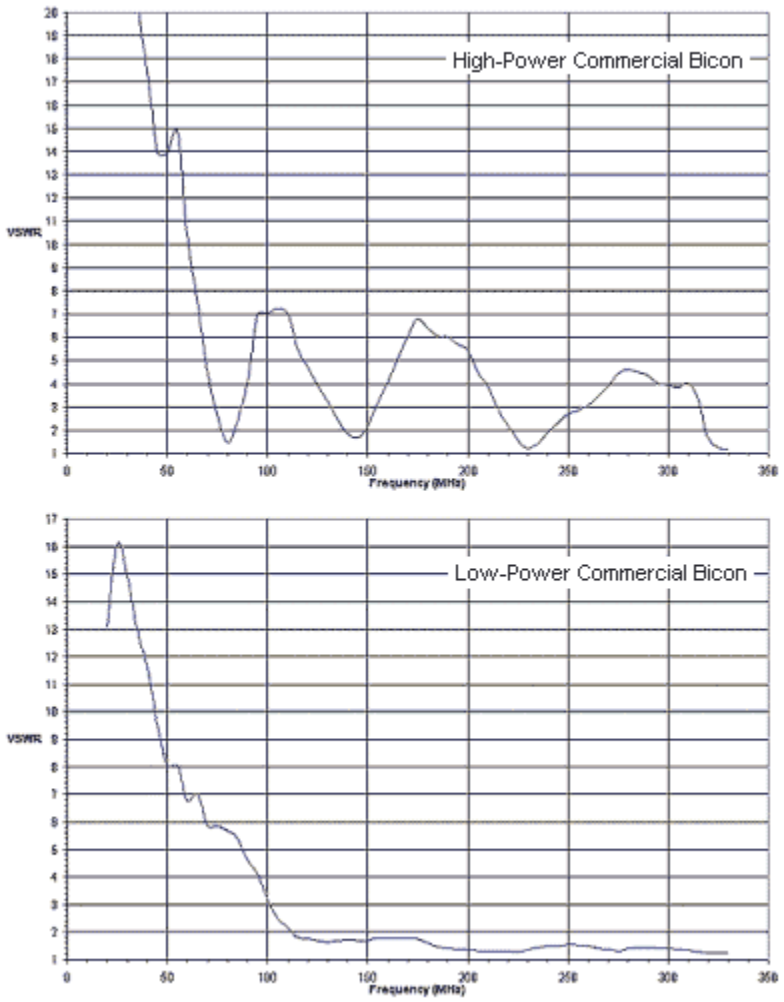

Typical Commercial Biconical Antenna SWR Curves

Although in most antenna work, we characterize antenna properties using the antenna structure alone, antennas intended for EMC testing tend to include in their characterizations the matching network normally built into the feedpoint. These networks may include any combination of inductive (transformer) and passive L-C network components. The matching networks may also include considerable losses, since each EMC antenna will also include a calibration chart. Since manufacturers normally do not specify in generally available data sheets the exact constituents of the matching network associated with the antenna, we can only infer the contents. For example, as a first order approximation, we may guess that the low-power biconical antenna includes considerable losses to result in the very low 50-Ω SWR above

100 MHz (with a presumed half-wavelength resonance of about 85 MHz). It is likely that the high-power antenna uses only a wide-band transformer, given the periodic peaks in the SWR curve.

We may simulate a rudimentary wide-band transformer using the NEC NT command with only shunt conductance values. I am indebted to Roy Lewallen for pointing me to the technique. As a sample case, I applied transformers with impedance ratios of 3:1 and 4:1 to the feedpoint of a 6-leg multi-center-wire closed-end 10° biconical antenna. I then ran 50-Ω SWR sweeps of the raw antenna and the antenna with each transformer. The results appear in **Fig. 12**.

Fig. 12

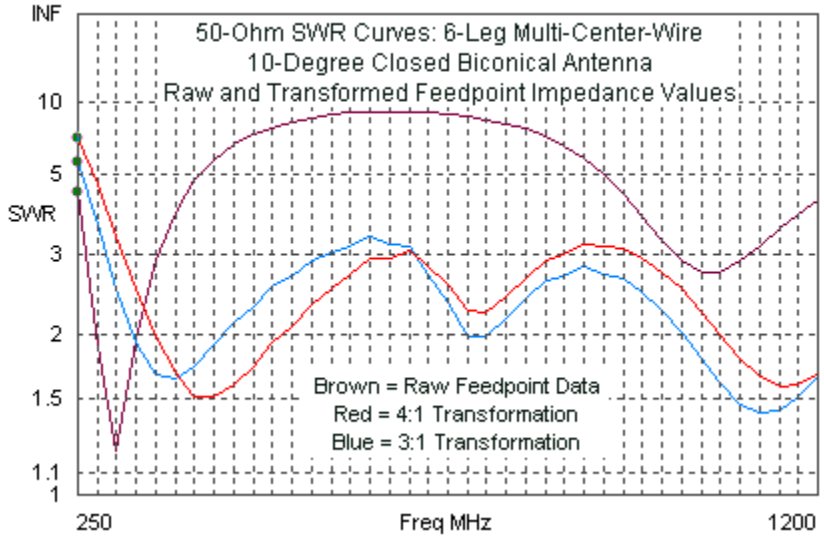

The curve for the unmatched antenna shows the design-frequency resonance at 300 MHz. By adding either transformer, we move the low-impedance SWR minimum upward in frequency, with a rapidly rising 50-Ω SWR value below the design frequency. This characteristic is similar to the situation that occurs with both SWR curves that are applicable to commercial antennas. Because the transformer in a NEC model is essentially lossless, the frequency range above the first low value will show periodic peaks. However, because a biconical antenna does not reach the peak values of either the resistive or reactive components of the feedpoint impedance that we find in a linear dipole when operated above its half-wavelength resonant frequency, the SWR peaks are much lower. In fact, if we could construct the requisite wide-band transformer and could handle 50-Ω SWR values of 3:1, the subject model would be usable as an ultra-wide-band antenna. Of course, that conclusion assumes at least a general level of model reliability.

The sample impedance transformation does not reflect the contents of the matching network of any actual EMC biconical antenna. I have presented it merely to suggest the means by which makers obtain low SWR values across wide frequency ranges in biconical antennas rated for EMC testing. For those not involved in EMC testing, it is important to note this specification sheet difference from what we normally encounter, that is, the raw or unmatched impedance characteristics of a subject antenna. (In fact, many Yagi antennas made for the amateur market include matching networks--typically gamma or beta networks--and provide the matched impedance SWR curves rather than the unmatched curves.) The distinction is also important when comparing broadband characteristics between antennas, especially where one may be an EMC antenna and the other a "raw" or unmatched antenna.

Conclusion

Biconical antennas, of course, have applications outside the realm of EMC testing. In such cases, their use is restricted ordinarily to the SWR passband defined for an unmatched or raw antenna. As the curves have shown, that range is very much larger than the passband at the same SWR limits for a linear dipole, but very much smaller than the range of an EMC antenna that includes matching and loss components.

This situation leads us back to the main goal of these notes: to ascertain the reliability of models of biconical antennas by using different methods of modeling. The use of a single center-section wire yields narrower modeled SWR passbands but a higher frequency for the -10-dB limiting frequency. The center section composed of multiple wires and using the NEC TL facility to feed each wire in parallel produces a wider SWR passband but a lower limiting frequency. The multiple-wire center section is attractive from a modeling perspective, since it yields a stable center-section length in models, a length that does not press NEC limits. However, whether it serves as the model that best replicates the physical reality of a biconical antenna requires comparison with chamber tests of actual biconical antennas constructed of materials similar to those used in the model.

Despite the limitations of the models, they are useful as a group in analyzing, at least as first-order approximations, the properties of actual biconical antennas. Although we cannot rely on the precise numbers produced by the models, we can make use of the general performance trends to understand better both the general performance of biconical antennas and some of their specific applications.